
Optical Properties of Langbeinites

III. Birefringence study at phase transitions and Raman scattering spectrums.

R.Vlokh, O.V.Vlokh, I.Skab, I.Girnyk

Institute of Physical Optics, laboratory of gradient optics, polarimetry and phase transitions, 23 Dragomanov Str., 79005, Lviv, Ukraine, e-mail:vlokh@ifp.lviv.ua

Received 15.11.2002

Abstract

The given part of this review paper is devoted to the collection and analysis of experimental results obtained by different researches that have investigated the temperature dependencies of birefringence as well as Raman scattering and IR spectrums of langbeinites at phase transitions. Given paper shows that optical methods of investigation of phase transitions particularly in langbeinites lead to obtaining important information about the temperature behavior of order parameter and lattice dynamic at phase transition. For example on the base of birefringence study of the isolated point of second order phase transition on the line of the first order was found on the concentration-temperature phase diagram of $K_2Cd_{2x}Mn_{2(1-x)}(SO_4)_3$ solid solutions. On the base of Raman scattering spectrums study one can conclude that phase transitions in langbeinites are of order-disorder type with ordering of the sulfate anions.

Key words: langbeinites, phase transition, Raman scattering, birefringence.

PACS: 42.33.SS-b.,77.80.B,78.20.Jq,78.30.-J

Contents

Introduction

1. Electrooptical effect (*in the previous issues*)
2. Optical activity and circular dichroism spectrums (*in the previous issues*)
3. Domain structure observation (*in the previous issues*)
4. Birefringence studying at phase transitions (*in the present issue*)
5. Raman scattering spectrums (*in the present issue*)

Conclusions

Introduction

One can obtain information about the character of phase transition from the result of the study of optical birefringence at phase transformations (see for example [1]). First of all it is possible to determine the order of phase transition, critical exponent of order parameter, proper or improper character of phase transition, etc. On the other

side the temperature evolution of IR and Raman scattering spectrums possesses the information about lattice dynamic and were usually studied for the determination of the microscopic origin of phase transition (see for example [2]). Both results of spectroscopic as well as crystalloptic investigations contain complementative data for the description of the structural transformations in solids.

The present report is devoted to the analysis of the results of crystalloptic and spectroscopy study of phase transitions in langbeinites.

4. Birefringence study at phase transitions

4.1. Birefringence study at the proper ferroelastic phase transitions

Investigation of the temperature dependence of birefringence in ferroelastic langbeinites was started from the potassium-cadmium compounds ($T_c=432\text{K}$, change of point group of symmetry at $T_c - 23\text{F}222$) [3]. From the obtained temperature dependencies (Fig. 1) one can conclude that phase transition in $\text{K}_2\text{Cd}_2(\text{SO}_4)_3$ crystals is of the first order but close to the second one.

Our study of temperature dependence of the birefringence [4,5] (Fig. 2) shows that at temperature $T_i=T_c-10\text{K}$ Δn_{31} possess a small anomaly. The change of phase of oscillation of the polarization ellipse at this temperature was also observed [4] (Fig. 3). It is interesting to note that temperature dependencies of the Δn_{12} and Δn_{23} do not manifest any anomaly at this temperature. On the other hand the relation

$$\Delta n_{12} + \Delta n_{23} + \Delta n_{31} = 1, \quad (1)$$

should be satisfactory for the principle values of

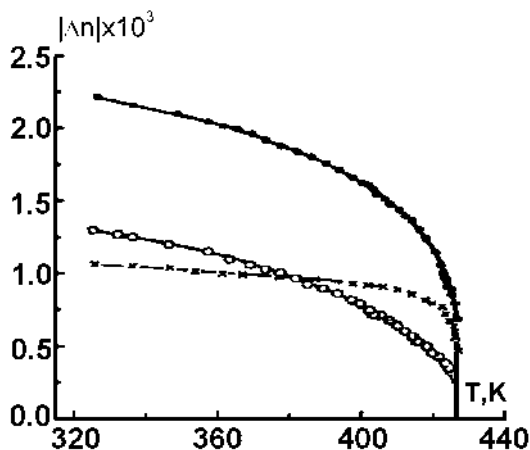


Fig. 1. Temperature dependencies of the birefringence of $\text{K}_2\text{Cd}_2(\text{SO}_4)_3$ crystals: 1- Δn_{23} ; 2- Δn_{31} ; 3- Δn_{12} [3].

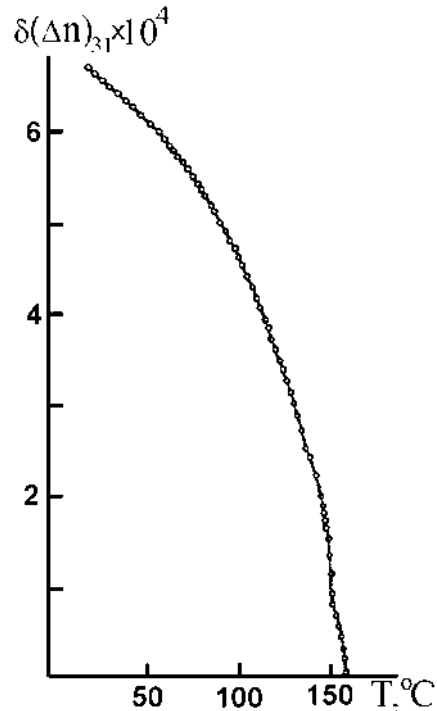


Fig. 2. Temperature dependence of the birefringence $\delta(\Delta n)_{31}$ in $\text{K}_2\text{Cd}_2(\text{SO}_4)_3$ crystals ($\lambda=632.8\text{nm}$) [4].

birefringence. It means that temperature T_i is not the temperature of some phase transition. As it follows from the results of temperature dependence of the lattice parameters [6], the b - parameter possesses the maximum at T_i i.e. at the increase of temperature the thermal expansion along b axis at T_i is changing to thermal compression. Such behavior of the lattice parameter b can effect the value of Δn_{31} measured by Senarmon method. In this case the measured temperature change of optical retardation can be written as

$$\frac{\partial(\Delta n_{31}d_b)}{\partial T} = d_b \frac{\partial \Delta n_{31}}{\partial T} + \Delta n_{31} \frac{\partial d_b}{\partial T}, \quad (2)$$

where d_b is the length of the sample along b axis. The second term in eq.(2) changes the sign at T_i and it leads to the existence of a small anomaly on the temperature dependence of measured birefringence that was calculated without taking into account the changing of d_b . The phase of oscillation of the ellipse of polarization also depends on retardation (Fig. 3).

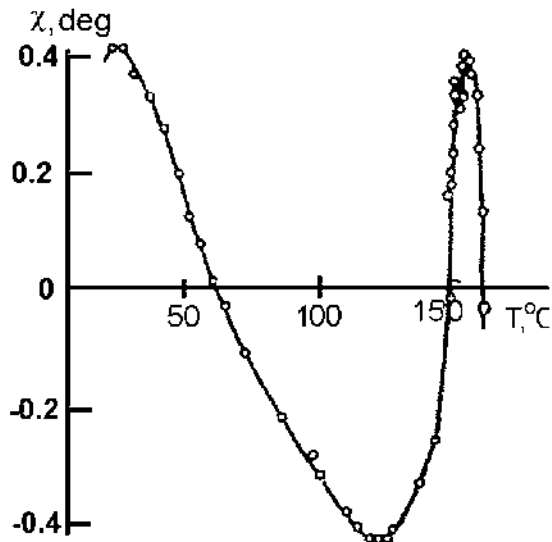


Fig. 3. Temperature dependence of the oscillation of ellipse polarization at light propagation along b -axis in $K_2Cd_2(SO_4)_3$ crystals ($\lambda=632.8\text{nm}$) [5].

The temperature dependence of birefringence was also investigated in $K_2Co_2(SO_4)_3$ crystals that possess a ferroelastic phase transition at $T_c=125\text{K}$ with a point group of symmetry change $23F222$ [7]. From these results (Fig. 4) it follows that phase transition in $K_2Co_2(SO_4)_3$ is also of the first order with the temperature hysteresis of T_c .

The temperature dependence of the birefringence at the ferroelastic phase transition was studied by us in $K_2Cd_{2x}Mn_{2(1-x)}(SO_4)_3$ solid

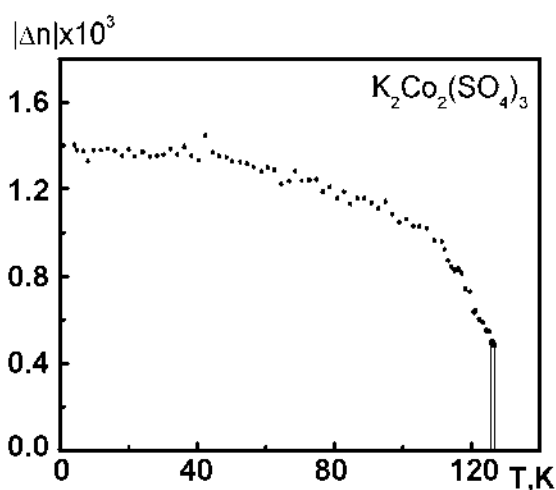


Fig. 4. Temperature dependence of the birefringence of $K_2Co_2(SO_4)_3$ crystals ($\lambda=643\text{nm}$, (100)-plate) [7].

solutions [8,9] (Fig. 5). In $K_2Mn_2(SO_4)_3$ and $K_2Cd_{0.4}Mn_{1.6}(SO_4)_3$ crystals birefringence appeared at the cooling rate with a jump-like change at $T_c=197\text{K}$ and $T_c=188\text{K}$, respectively, and then increased at $T < T_c$. In $K_2Cd_{0.2}Mn_{1.8}(SO_4)_3$ and $K_2Cd_{1.0}Mn_{1.0}(SO_4)_3$ mixed crystals birefringence appeared at the cooling rate at $T_c=175\text{K}$ and $T_c=250\text{K}$, respectively. For both crystals linear temperature behavior of the birefringence started from $T=165\text{K}$ (for $x=0.1$) and $T=230\text{K}$ (for $x=0.5$). Such temperature behavior of the birefringence means that the temperature regions $165\text{K} < T < 175\text{K}$ and $230\text{K} < T < 250\text{K}$ are the regions of the diffusion of phase transitions of the first order. In the $K_2Cd_{1.4}Mn_{0.6}(SO_4)_3$ and $K_2Cd_{1.8}Mn_{0.2}(SO_4)_3$ crystals birefringence decreases gradually at the heating rate and disappears at $T_c=346\text{K}$ and $T_c=386\text{K}$, respectively. Such temperature behavior of the optical birefringence means that phase transitions in the mixed crystals with $x=0.7$ and $x=0.9$ may be of the first order but nearer to the second order. In $K_2Cd_2(SO_4)_3$ crystals we observed the jump-like changing of the birefringence at the first order phase transition point ($T_c=432\text{K}$). Contrary to all the mentioned cases the $K_2Cd_{1.6}Mn_{0.4}(SO_4)_3$ solid solutions possess the second order phase transition. The birefringence disappeared at $T_c=358\text{K}$ in heating rate.

4.2. Birefringence study in ferroelectric langbeinites

The temperature dependence of birefringence at the ferroelectric phase transition in langbeinites was studied in $(NH_4)_2Cd_2(SO_4)_3$ and $Rb_2Cd_2(SO_4)_3$ crystals [10, 11]. The temperature dependencies of birefringence Δn_{12} and optical indicatrix rotation angle are presented on Fig. 6 [10].

The results presented on Figure 6 were described on the base of a thermodynamic approach taking into account the improper nature of the ferroelectric phase transition in

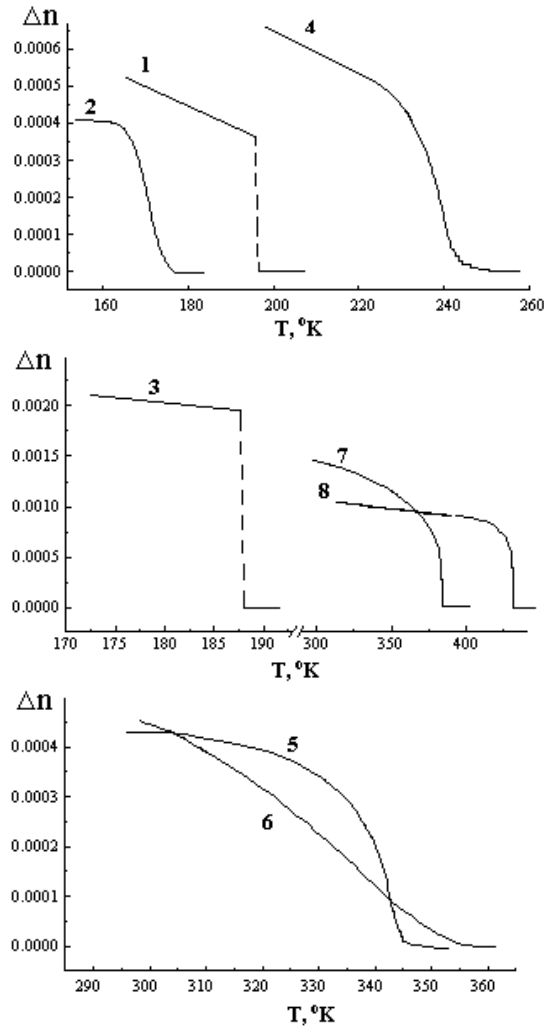


Fig. 5. The temperature dependencies of the birefringence at ferroelastic phase transition in $K_2Cd_{2x}Mn_{2(1-x)}(SO_4)_3$ solid solutions ($\lambda=632.8nm$) [8,9]:

- | | | |
|-------------------------------------|-------------------------------------|-------------------------------------|
| 1 - $K_2Mn_2(SO_4)_3$; | 4 - $K_2Cd_{1.0}Mn_{1.0}(SO_4)_3$; | 7 - $K_2Cd_{1.8}Mn_{0.2}(SO_4)_3$; |
| 2 - $K_2Cd_{0.2}Mn_{1.8}(SO_4)_3$; | 5 - $K_2Cd_{1.4}Mn_{0.6}(SO_4)_3$; | 8 - $K_2Cd_2(SO_4)_3$ |
| 3 - $K_2Cd_{0.4}Mn_{1.6}(SO_4)_3$; | 6 - $K_2Cd_{1.6}Mn_{0.4}(SO_4)_3$; | |

$(NH_4)_2Cd_2(SO_4)_3$ crystals [10]. The thermodynamic potential for the phase transition 23F2 in langbeinites is [12, 13]

$$G = G_0 + \frac{1}{2}\alpha(q_1^2 + q_2^2) + \frac{1}{4}\beta_1(q_1^4 + q_2^4) + \frac{1}{2}\beta_2q_1^2q_2^2 + \frac{1}{6}\xi(q_1^2 + q_2^2)^3 + \frac{1}{2}\mu P_3q_1q_2 + \frac{1}{2}\gamma P_3^2(q_1^2 + q_2^2) + \frac{1}{2}\kappa P_3^2 \quad (3)$$

where q_1, q_2 are the components of the order parameter and P_3 - spontaneous polarization. From eq.(3) it is possible to derive all necessary parameters for describing the results presented

in Fig. 6: polarization coefficient

$$\Delta B_6 = \omega_1q_1q_2 + \omega_2P_3(q_1^2 + q_2^2) + r_{63}P_3, \quad (4)$$

spontaneous polarization

$$P_{3s} = -\frac{\mu q_{1s}q_{2s}}{\kappa + \gamma(q_{1s}^2 + q_{2s}^2)}, \quad q_{1s}^2 = q_{2s}^2 \quad (5)$$

spontaneous change of polarization constant and electrooptical coefficient

$$\Delta B_{6s} = (r_{63} - D)P_{3s} \quad (6)$$

$$r_{63}^f = r_{63}^p + D\left(\frac{\kappa_p}{\kappa_f} - D\frac{\mu\kappa_p}{\omega_1}\right), \quad (7)$$

where

$$D = \frac{\omega_1}{\kappa_p (\mu + 2\gamma P_{3s})}, \quad (8)$$

and susceptibilities $\kappa_p = \frac{1}{\kappa}$ for $T > T_c$ and

$$\kappa_f = \frac{\kappa + 2\gamma q_{1s}^2 - \mu^2 \kappa^2}{(\beta_1 + \beta_2 + 8\xi q_{1s}^2)(\kappa + 2\gamma q_{1s}^2)^2} \quad (9)$$

for $T < T_c$

For proper ferroelectrics $\Delta B_{6s} = r_{63}^p P_{3s}$ and $r_{63}^f = r_{63}^p$, so that $D=0$. Thus the quantity D makes the contribution of an actual order parameter to the birefringence and electrooptical coefficient in the ferroelectric phase (temperature dependence of the electrooptical coefficient was also presented in [10]). On the base of the above mentioned relations the authors of [10] have been compared the results of calculation with experiments (Fig. 7).

From the results of the experiment and calculation it is clearly visible that the temperature dependence of birefringence in $(NH_4)_2Cd_2(SO_4)_3$ crystals is determined both by the order parameter as well as spontaneous polarization making the order of a smaller contribution to the birefringence in the ferroelectric phase than it is observed experimentally.

From our results of the study of the temperature dependence of birefringence (Fig. 8) [11] and domain structure [14] of $Rb_2Cd_2(SO_4)_3$ crystals it follows that temperature $T_c=113K$ is the temperature of phase transition with the change of symmetry 23F3. We would like to note that the existence of a trigonal phase was observed in langbeinites for the first time.

5. Raman scattering spectrums

The first results of study of the vibration spectra of the langbeinites were obtained by R.Brown and D.Ross [15]. The authors have obtained the IR spectra of 26 langbeinite compounds $M_2^I M_2^{II}(SO_4)_3$ in the region of $4000\sim 40cm^{-1}$ and interpreted in terms of the vibration of SO_4

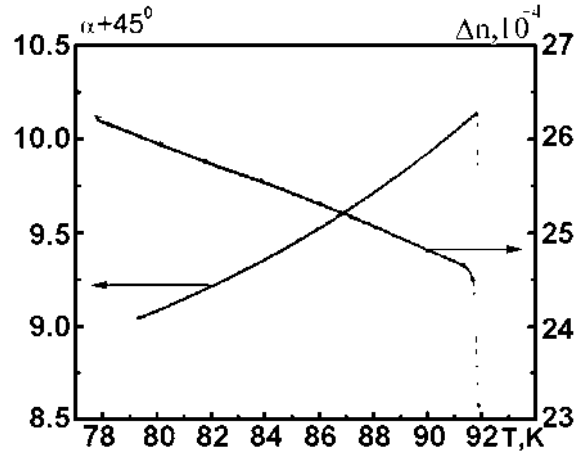


Fig. 6. Temperature dependence of birefringence Δn_{12} and optical indicatrix rotation angle in $(NH_4)_2Cd_2(SO_4)_3$ crystals.

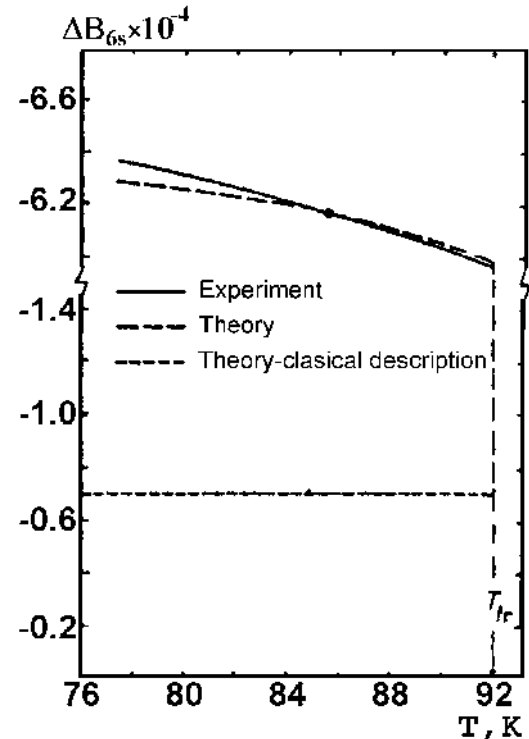


Fig. 7. Temperature dependence of ΔB_{6s} . Solid line - ΔB_{6s} calculated from the experimental results (Fig.6) by the formula

$$\Delta B_{6s} = \frac{1}{n_o^3} \frac{2 \tan^2 2\alpha}{1 + 2 \tan^2 2\alpha} \Delta n_{12}.$$

Dashed line - ΔB_{6s} calculated from the theoretical expressions (6) and (8). Dotted line - ΔB_{6s} calculated from (6) with $D=0$ [10] crystals [10].

tetrahedra and $M^{II}O_6$ octahedra. The following reports were devoted to the study of the Raman spectra of langbeinites at phase transitions [16-21]. Almost simultaneously Raman spectra were

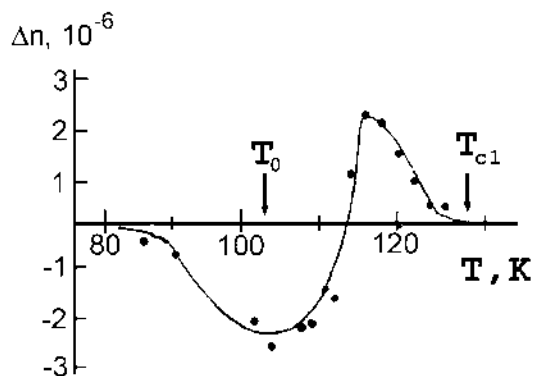


Fig. 8. Temperature dependence of birefringence in $\text{Rb}_2\text{Cd}_2(\text{SO}_4)_3$ crystals ($\lambda=632.8\text{nm}$) [11].

obtained for $(\text{NH}_4)_2\text{Cd}_2(\text{SO}_4)_3$, $(\text{ND}_4)_2\text{Cd}_2(\text{SO}_4)_3$ and $\text{Tl}_2\text{Cd}_2(\text{SO}_4)_3$ by L.Rabkin et al [16] and for $\text{K}_2\text{Mn}_2(\text{SO}_4)_3$, $(\text{NH}_4)\text{Cd}_2(\text{SO}_4)_3$, and $\text{Tl}_2\text{Cd}_2(\text{SO}_4)_3$ by S.Kreske and V.Devarajan [17]. In [17] complete vibrational spectra (Raman, IR and far IR) for the ferroelastic ($\text{K}_2\text{Mn}_2(\text{SO}_4)_3$) and ferroelectric ($(\text{NH}_4)_2\text{Cd}_2(\text{SO}_4)_3$, and $\text{Tl}_2\text{Cd}_2(\text{SO}_4)_3$) langbeinites were obtained. Authors have identified and assigned the various symmetry species of the paraphase factor group T for all the crystals the vibrational modes, corresponding to the “internal” vibrations of $(\text{SO}_4)^{2-}$ ion in the polarized single-crystal Raman spectra. Raman spectra were recorded at various temperatures down to the liquid nitrogen temperature. According to the authors [17] no soft modes were observed near the phase transitions. But abrupt changes in the slopes of full width and half maximum versus temperature and peak high versus temperature, corresponding to the Raman-active $(\text{SO}_4)^{2-}$ internal vibrations were seen near the phase transitions. This indicates the probability of an order-disorder phase transition mechanism involving the $(\text{SO}_4)^{2-}$ ions. In the monoclinic and triclinic phases of $\text{Tl}_2\text{Cd}_2(\text{SO}_4)_3$ crystals cell doubling was not observed.

The Raman spectrum of $(\text{NH}_4)_2\text{Cd}_2(\text{SO}_4)_3$, $(\text{ND}_4)_2\text{Cd}_2(\text{SO}_4)_3$ and $\text{Tl}_2\text{Cd}_2(\text{SO}_4)_3$ crystals where studied in [16] in the temperature range covered all phase transitions. In the

$\text{Tl}_2\text{Cd}_2(\text{SO}_4)_3$ crystals the anomaly band with the E symmetry was observed frequently with a decrease from 17cm^{-1} at 25°C down to 5cm^{-1} at the vicinity of phase transition to the monoclinic phase (Fig. 9).

This line corresponds to the double degenerated soft mode, described by two-dimensional irreducible representation of $P2_13$ group of symmetry for Γ -point ($k=0$) of Brillouin zone. On the other hand phase transitions to the $R3$, $P2_1$ and $P1$ space group of symmetry can be effected by the lattice instability in respect to the double degenerated soft phonon in M -point of Brillouin zone or can be induced by the six component order parameter of X -point. In both cases the two or four times multiplication of the unit cell volume

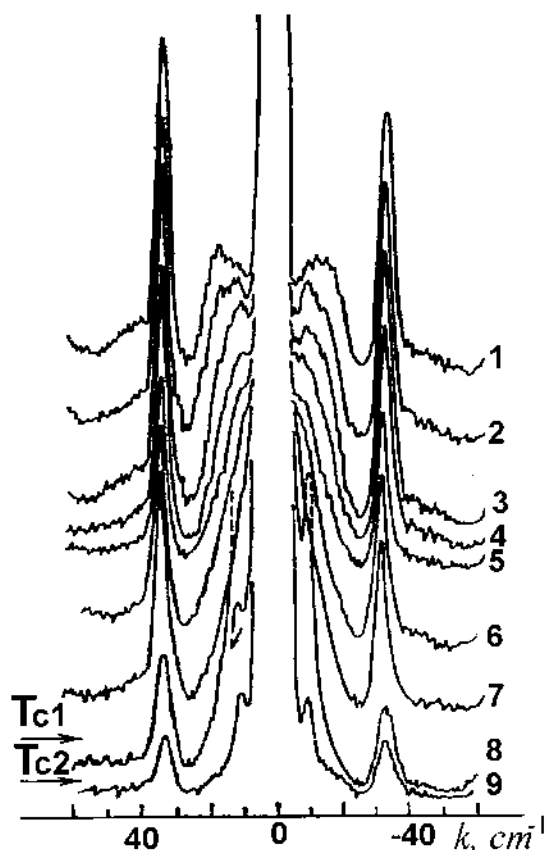


Fig. 9. Temperature behavior of the low frequency Raman spectra of $\text{Tl}_2\text{Cd}_2(\text{SO}_4)_3$ crystals ($z(xx)y$ -orientation): 1- $T=-20^\circ\text{C}$, 2- $T=-45^\circ\text{C}$, 3- $T=-65^\circ\text{C}$, 4- $T=-85^\circ\text{C}$, 5- $T=-105^\circ\text{C}$, 6- $T=-120^\circ\text{C}$, 7- $T=-143^\circ\text{C}$, 8- $T=-147^\circ\text{C}$, 9- $T=-156^\circ\text{C}$ [16].

should be observed and soft mode cannot exist in the cubic phase in the first order scattering.

Any soft modes were observed in $(\text{ND}_4)_2\text{Cd}_2(\text{SO}_4)_3$ and $(\text{NH}_4)_2\text{Cd}_2(\text{SO}_4)_3$ crystals (see for example Fig. 10)[16].

Since spectra of $\text{Tl}_2\text{Cd}_2(\text{SO}_4)_3$ and $(\text{NH}_4)_2\text{Cd}_2(\text{SO}_4)_3$ crystals in orthorhombic and monoclinic phases respectively are similar, authors of [16] come to the conclusion that there is no great difference between the energies of these phases.

Raman spectra of $\text{K}_2\text{Cd}_2(\text{SO}_4)_3$ crystals have been studied in [18] (Fig. 11). The above phase transition temperature (159°C) only one wide band with the frequency 38cm^{-1} was observed. This band does not change their frequency and intensity at heating up to 200°C . Any line that can be identified as a soft mode was not observed.

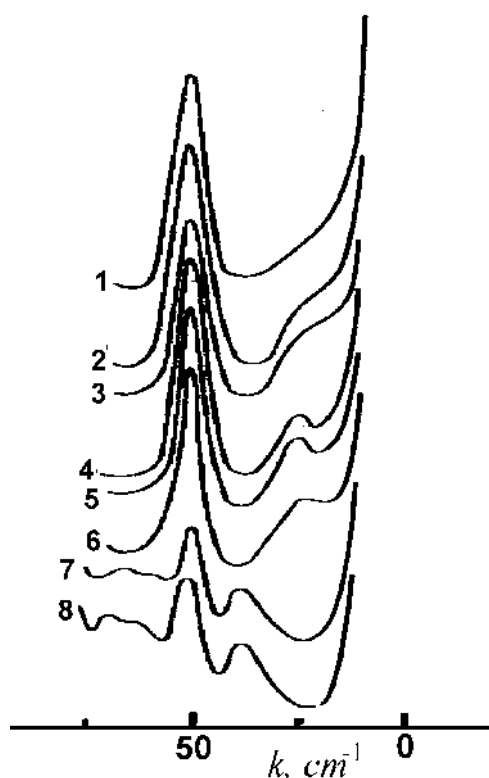


Fig. 10. Temperature behavior of the low frequency Raman spectra of $(\text{NH}_4)_2\text{Cd}_2(\text{SO}_4)_3$ crystals ($z(xx)y$ -orientation):
 1– $T = -160^\circ\text{C}$, 2– $T = -164^\circ\text{C}$, 3– $T = -168^\circ\text{C}$,
 4– $T = -171^\circ\text{C}$, 5– $T = -177^\circ\text{C}$, 6– $T = -179^\circ\text{C}$,
 7– $T = -185^\circ\text{C}$, 8– $T = -190^\circ\text{C}$ [16].

The low frequency Raman spectrums of $\text{Rb}_2\text{Cd}_2(\text{SO}_4)_3$ crystals are shown on Fig. 12, [19]. In these spectrums the softening of the E -line (20cm^{-1} at 25°C) is observed. This mode decreases its frequency with the decrease of the temperature and already at 50°C above the first phase transition is shifted to the Rayleigh band. Thus this mode possesses a relaxation behavior. As well as in the previous cases any from the observed modes in $\text{Rb}_2\text{Cd}_2(\text{SO}_4)_3$ and also in $\text{K}_2\text{Co}_2(\text{SO}_4)_3$ [20] crystals can not be identified as a soft mode.

The authors of [21] studied the Raman scattering spectrums in $(\text{NH}_4)_2\text{Ni}_2(\text{SO}_4)_3$ and $\text{K}_2\text{Ni}_2(\text{SO}_4)_3$ crystals. They found that $\text{K}_2\text{Ni}_2(\text{SO}_4)_3$ crystals possess the phase transition at 113°C probably of the order-disorder type.

Interesting results were obtained in [22] by the method of micro-Raman scattering in

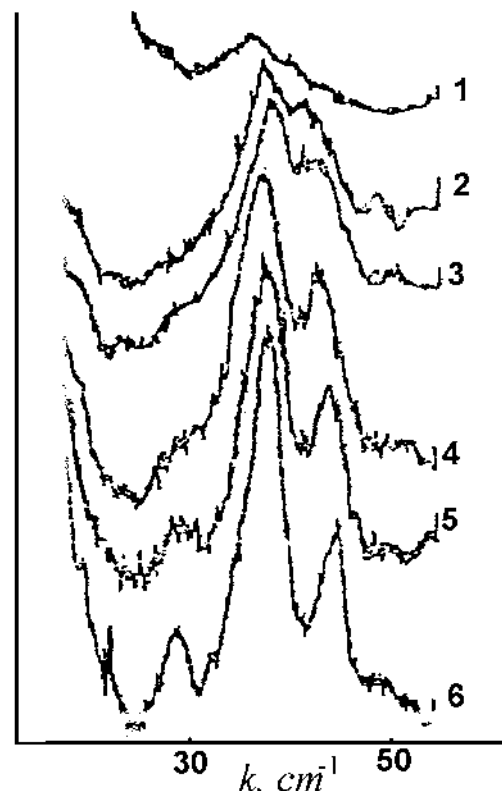


Fig. 11. Temperature behavior of the low frequency Raman spectra of $\text{K}_2\text{Cd}_2(\text{SO}_4)_3$ crystals ($x(zz)y$ -orientation):
 1– $T = 177^\circ\text{C}$, 2– $T = 142^\circ\text{C}$, 3– $T = 123^\circ\text{C}$,
 4– $T = 107^\circ\text{C}$, 5– $T = 80^\circ\text{C}$, 6– $T = 22^\circ\text{C}$ [18].

$K_2Mn_2(SO_4)_3$ crystals. A micro-Raman mapping study was carried out near the transition temperature. The spectra exhibit either the high-temperature phase or low-temperature phase structure. It is concluded that the sample crystals consist of local regions that have different transition temperatures. Results obtained in [22] indicate that not an intermediate phase but a coexistence of two phases appear in the $K_2Mn_2(SO_4)_3$ crystals. Results reported in [22] are in good agreement with our data of microscopic observation of phase transition temperature evolution and the appearance of a "forbidden" domain structure in $K_2Mn_2(SO_4)_3$ crystals [9, 23].

The hypothetical phase diagram for langbeinite crystals (Fig. 13) was obtained in [24] on the base of analyzing thermodynamic potential expanded by two strongly interacting order parameters

$$F = a_1\eta^2 + a_2\eta^4 + b_1\xi^2 + b_2\xi^4 + \gamma_1\xi\eta^2 + \gamma_2\xi^2\eta^2. \quad (10)$$

Assuming that coefficients a_i and b_i in eq.(10) linearly depend on temperature, then the temperature axis in Figure 13 will be represented as a straight line. The disposition of this line on the plane (a_i, b_i) should determine the sequence of phase transition in the chosen langbeinite crystal. Thus the thermodynamic

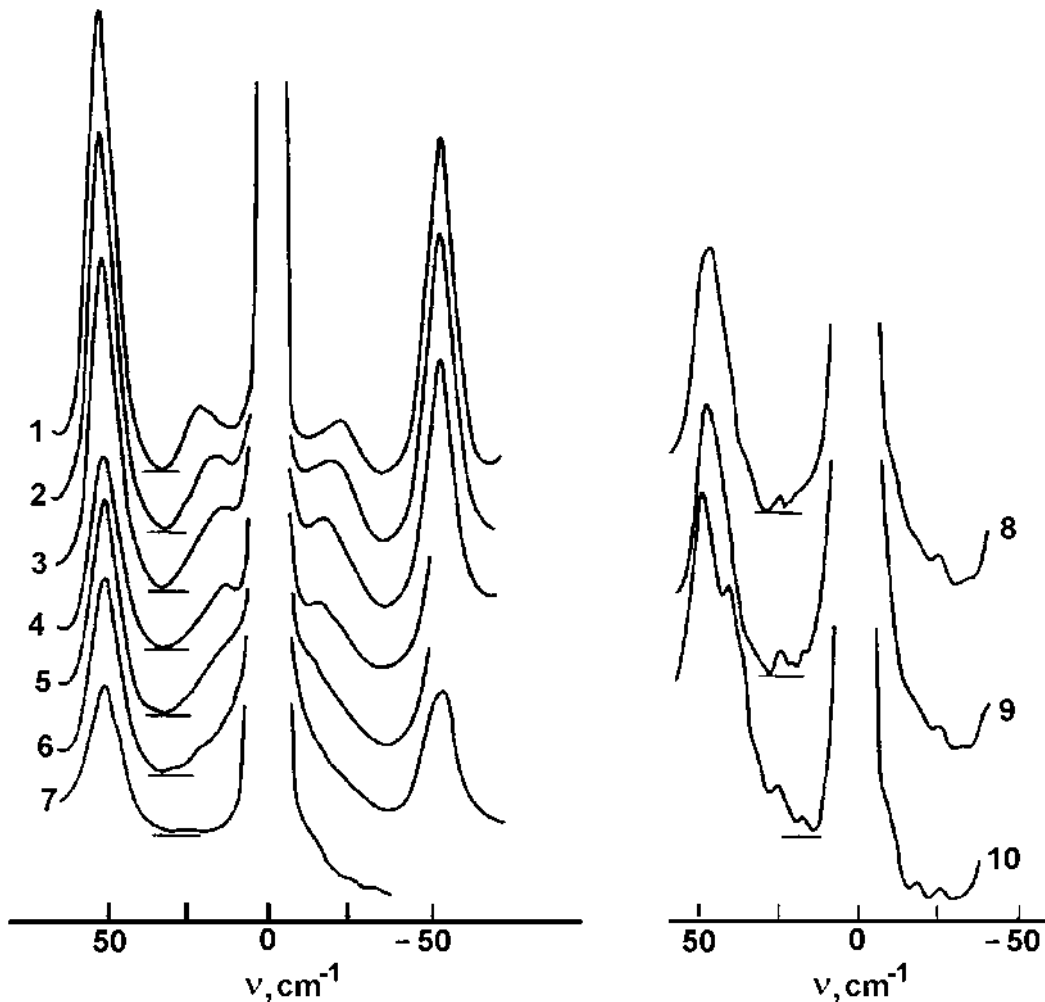


Fig. 12. Temperature behavior of the low frequency Raman spectra of $Rb_2Cd_2(SO_4)_3$ crystals ($z(y'x')y'$ -orientation): 1- $T=20^\circ C$, 2- $T=-5^\circ C$, 3- $T=-33^\circ C$, 4- $T=-63^\circ C$, 5- $T=-93^\circ C$, 6- $T=-134^\circ C$, 7- $T=-155^\circ C$; ($z(xx)y$ -orientation): 8- $T=-160^\circ C$, 9- $T=-161^\circ C$, 10- $T=-185^\circ C$ [16].

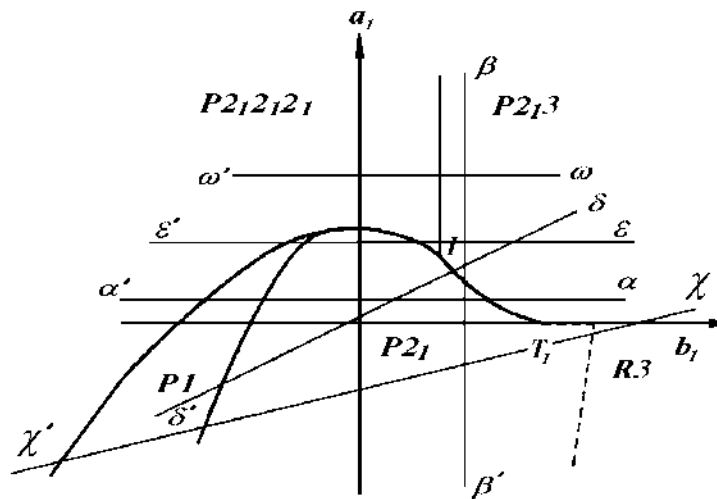


Fig. 13. Hypothetical phase diagram for the langbeinite crystals [24].

way $\omega-\omega'$ is observed in $K_2Mn_2(SO_4)_3$, $K_2Co_2(SO_4)_3$ and $K_2Cd_2(SO_4)_3$ ferroelastic crystals; the thermodynamic way $\beta-\beta'$ characterizes $(NH_4)_2Cd_2(SO_4)_3$ crystals which undergo only one phase transition with the change of symmetry $P2_13 \rightarrow P2_1$; $Tl_2Cd_2(SO_4)_3$ crystals possess the thermodynamic way $\alpha-\alpha'$ that undergo phase transitions with the change of symmetry $P2_13 \rightarrow P2_1 \rightarrow P1 \rightarrow P2_12_12_1$. According to the authors $Rb_2Cd_2(SO_4)_3$ crystals possess thermodynamic way $\delta-\delta'$. But according to our observation of domain structure and dielectric measurements $Rb_2Cd_2(SO_4)_3$ crystals should possess the thermodynamic way $\chi-\chi'$ with the manifestation of all possible phases of langbeinites $P2_13 \rightarrow R3 \rightarrow P2_1 \rightarrow P1 \rightarrow P2_12_12_1$. Moreover in the $Tl_{2x}Rb_{2(1-x)}Cd_2(SO_4)_3$ the predicted tricritical point T_I could be observed. The thermodynamical way $\varepsilon-\varepsilon'$ was never observed in langbeinites, but probably this way could exist in $K_{2x}Tl_{2(1-x)}Cd_2(SO_4)_3$ (change of symmetry $P2_13 \rightarrow P2_12_12_1 \rightarrow P2_1 \rightarrow P1 \rightarrow P2_12_12_1$) solid solutions with a manifestation of triple point I .

Conclusions

To part I

1. On the base of the analysis of the polarizability of cations and anions F. Emmenegger et al come to the conclusion that

the principal contribution to the electrooptical effect comes from the sulfate ions. For the manganese compounds, with the exception of $(NH_4)_2Mn_2(SO_4)_3$ crystals electrooptical power is found to be approximately constant. Its value appears to increase as the polarizability of the univalent ion increases, which implies that univalent ions make a small contribution to the electrooptical effect with the same sign as that of the sulfate contribution. For the ammonium compound the electrooptical effect is nearly zero. It means that unlike the other univalent cations, the highly acentrosymmetric ammonium ion makes a large contribution nearly equal in magnitude to that of the sulfate ion and opposite in sign. The difference of electrooptical power for the $K_2Mn_2(SO_4)_3$ and $K_2Ni_2(SO_4)_3$ suggests that the divalent ions also contribute significantly to the electrooptical effect. But this conclusion is not in agreement with the result of a study of the electrooptical effect in $(NH_4)_2Cd_2(SO_4)_3$ crystals. It means that the conclusion about the opposite sign of contributions to electrooptical effect from ammonium and sulfate groups is premature and microscopic theory of electrooptical properties of this family of crystals is not yet developed.

2. On the base of a study of the dispersion of optical activity, absorption spectrums and spectrums of circular dichroism it was

concluded that optical activity in langbeinites possesses a “molecular” nature and appears as the result of interactions in the SO_4^{2-} tetrahedrons with the symmetry C_1 .

To part II

1. Using a polarisation microscope we observed the appearance of domain structure in all $\text{K}_2\text{Cd}_{2x}\text{Mn}_{2(1-x)}(\text{SO}_4)_3$ solid solutions. These domains are separated by thick walls with an average thickness of 16-40 μm for $\text{K}_2\text{Cd}_2(\text{SO}_4)_3$ crystals. The domain walls were not planer and were almost parallel to the $\{110\}$ planes. The region of domain walls belongs to the paraelastic cubic phase. The domain walls in $\text{K}_2\text{Cd}_{1.6}\text{Mn}_{0.4}(\text{SO}_4)_3$ compounds, which belong to an isolated point, are planer thin walls with an orientation (110) and $(\bar{1}10)$. The origin of the multidomain-heterophase structure is discussed phenomenologically based on the prototype phase with point group of symmetry $\bar{4}3m$. In this case there are two modifications in the system with point group 23 related by $\bar{4}$ and m_d symmetry elements which transform the coordinate system (xyz) to (yxz) . Six enantiomorphic domains can exist in the 222 phase (three right and three left domains) and between some of them, domain walls with $\{110\}$ orientation can occur, if the coefficients of thermodynamic potential near the third order term δ_1 vanish. This fact follows from X-ray data for pure $\text{K}_2\text{Cd}_2(\text{SO}_4)_3$ and $\text{K}_2\text{Mn}_2(\text{SO}_4)_3$ crystals. For the crystals which belong to the isolated point the coefficient $\delta_1=0$. Our investigations show that the relation between coefficients of the thermodynamic potential plays an important role in the formation of the forbidden domain structure. The investigation of the optical activity shows the change of sign of optical rotary power in some regions of samples in the 23 symmetry phase of $\text{K}_2\text{Cd}_{2x}\text{Mn}_{2(1-x)}(\text{SO}_4)_3$ crystals. It means that in the phase with symmetry 23 enantiomorphic twinning exists and langbeinites possess the prototype phase with point group of symmetry $\bar{4}3m$. The

domain structure of the $\text{K}_2\text{Co}_2(\text{SO}_4)_3$ ferroelastics is similar to the above-mentioned.

2. The appearance of a trigonal phase with point group of symmetry 3 was found between cubic and monoclinic phases of $\text{Rb}_2\text{Cd}_2(\text{SO}_4)_3$ crystals by studying the domain structure. It was found also that trigonal and monoclinic phases coexist in these compounds.

To part III

1. The concentration-temperature phase diagram for $\text{K}_2\text{Cd}_{2x}\text{Mn}_{2(1-x)}(\text{SO}_4)_3$ solid solutions was obtained by studying of the optical birefringence and domain structure of $\text{K}_2\text{Cd}_{2x}\text{Mn}_{2(1-x)}(\text{SO}_4)_3$ solid solutions. The isolated point of the second order phase transition ($x=0.8$; $T_i=358\text{K}$) has been found on the line of the first order phase transitions $T_c(x)$. The study of the birefringence of $(\text{NH}_4)_2\text{Cd}_2(\text{SO}_4)_3$ crystals shows an improper nature of the ferroelectric phase transition in these crystals.

2. The study of the Raman spectra of langbeinites shows that any line can not be identified as a soft mode. Thus phase transitions in this crystal family are of the order-disorder type.

References

1. Fousek J. Phys.Stat.Sol.(a) 55 (1979) 11.
2. Lines M.E., Glass A.M. Principle and Application of Ferroelectrics and Related Materials. Clarendon Press, Oxford (1977).
3. Pozdeev V.G. Crystallography 27 (1982) 1196 (in Russian).
4. Vlokh O.G., Vlokh R.O., Shopa Ya.I. Ukr.J.Phys. 32 (1987) 1040 (in Russian).
5. Bilecky I.N., Vlokh R.O., Otko A.I., Shopa Ya.I. Ukr.J.Phys. 33 (1988) 689 (in Russian).
6. Lissalde F., Abrahams S.C., Bernstein J.L. and Nassau K. J.Appl.Phys. 50 (1979) 845.
7. Brezina B., Rivera J.-P., Schmid H. Ferroelectrics 55 (1984) 177.
8. Vlokh R., Vlokh O.V., Skab I.P., Romanyuk M.O. Ukr.J. of Phys. 43 (1989) 80 (in Ukrainian).

9. Vlokh R., Czapla Z., Kosturek B., Skab I., Vlokh O.V. Girnyk I. *Ferroelectrics* **219** (1998) 243.
10. Konak C., Fousek J., Ivanov N.R. *Ferroelectrics* **6** (1974) 235.
11. Vlokh R., Skab I., Guzandrov A., Mogylyak I., Smaglyi S., Uesu Y. *Ferroelectrics*, **237** (2000) 489.
12. Dvorak V. *Phys. Stat. Sol. (b)* **52** (1972) 93.
13. Dvorak V. *Phys. Stat. Sol. (b)* **66** (1974) K87.
14. Vlokh R., Skab I., Girnyk I., Czapla Z., Dacko S., Kosturek B. *Ukr.J.Phys.Opt.* **1** (2000) 103.
15. Brown R., Ross D. *Spectrochimica Acta* **26A** (1970) 1149.
16. Rabkin L., Torgashev V., Latush L., Brezina B., Shuvalov L. *Crystallography* **24** (1979) 487 (in Russian).
17. Kreske S., Devarajan V. *J.Phys.C:Solid State Phys.* **15** (1982) 7333.
18. Moiseenko V., Pozdeev V., Pastukhov V. *Sol.Stat.Phys.* **25** (1983) 2191 (in Russian).
19. Latush L., Rabkin L., Torgashev V., Yuzyuk Yu., Shuvalov L., Brezina B. *Crystallography* **29** (1984) 945 (in Russian).
20. Rabkin L., Rychkov G., Torgashev V., Yuzyuk Yu., Brezina B. *Crystallography* **30** (1985) 599 (in Russian).
21. Jayakumar V.S., Hubert Joe I., Aruldas G. *Ferroelectrics* **165** (1995) 307.
22. Sakai A., Inagaki T., Moriyoshi C., Itoh K. *Ferroelectrics* **272** (2002) 27.
23. Vlokh R., Skab I., Vlokh O., Uesu Y. *Ukr.J.Phys.Opt.* **2** (2001) 148.
24. Latush L., Rabkin L., Torgashev V., Shuvalov L. Brezina B. *News of Acad.Sc.USSR* **47** (1983) 476 (in Russian).